Implantable Magnetic Glass−Ceramic Based on $(Fe,Ca)SiO_3$ Solid Solutions

R. P. del Real, D. Arcos, and M. Vallet-Regí*

Dpto. de Química Inorgánica y Bioinorgánica, Facultad de Farmacia, Universidad Complutense, 28040-Madrid, Spain

Received January 30, 2001. Revised Manuscript Received October 8, 2001

A magnetic glass−ceramic suitable to be used as biomaterial has been synthesized. After the $NaO-Fe_2O_3-CaO-SiO_2$ starting glass is annealed, a glass−ceramic based on ferroan wollastonite-like and ϵ-$(Fe,Ca)SiO_3$-like phases is obtained. Both phases contain Fe^{2+} ions, leading to two magnetic phases with different coercive forces. Because of the magnetic properties, this material could be used as a thermoseed for cancer treatment by hyperthermia. This glass−ceramic is coated by an amorphous layer when it is soaked in simulated body fluid (SBF). This new layer, formed with the incorporation of phosphorus over the surface, would lead to a good integration with the bone tissue after being implanted.

Introduction

Hyperthermia is a cancer therapy which consists of heating target tissues to temperatures between 41 and 46 °C. Malignant cells appear to be selectively destroyed in this range of temperatures, mainly by induced cytoplasmic damage.[1] Although there is no individual cellular target of hyperthermia, an increase of the lysosomal activation and a relative increase in the anaerobic glycolysis with respect to the oxygen metabolism lead to higher acidity conditions and therefore to tumor cell destruction. This selective damage seems to be due to the environment of the tumor cells, such as hypoxia and insufficient nutrition as a consequence of the abnormal architecture of tumor blood vessels.

Today, many cellular factors are known to be important in cell inactivation.[2] Different effects such as thermotolerance, induced apoptosis, changes of microvascularization, or better recognition of the cancerous cells by the natural killer cells after hyperthermia treatment have important roles in this kind of therapy.[3−6]

One of the main problems in hyperthermia treatment is the development of techniques for the establishment of hyperthermic conditions in human tumors. Actually, heat focusing, homogeneous heating, and the influence of the blood flow or the tumor geometry are well-known limitations.[7,8] In this sense, several strategies such as self-regulating thermoseeds, new designs for the energy sources, or modeling and computer simulation are considered to improve the effectiveness of this cancer therapy.[9−15]

Ferromagnetic materials are expected to be useful as thermoseeds for hyperthermia treatment of cancer. When they are implanted and an alternating magnetic field is applied, they heat the tissues by means of magnetic losses.[16] Several methods have been used for hyperthermia therapy. Metals such as iron, copper, and aluminum, and alloys such as steel 41, stainless steel 430, or palladium−cobalt alloys are useful as heating elements.[9,12] An implantable heater consisting of a rod of ferrite and a metal ring has been tested as another kind of induction heating method, showing very good accuracy of the heating regulation.[17] Since metals are exposed to corrosion inside the body, they are especially useful against tumors that are not deeply seated, for example in the intraoral cavity.

A possibility to treat internal tumors is to use injectable ferrofluids containing magnetite particles. This therapy has been reported to be effective against several tumors such as solid glicoma, human lung adenocarcinoma cells, mammary carcinoma, and so forth.[18−21]

* Author to whom correspondence should be addressed

(1) Overgaard, J. *Cancer* **1977**, *39*, 2637.
(2) Jordan, A.; Scholz, R.; Wust, P.; Fähling, H.; Felix, R. *J. Magn. Magn. Mater.* **1999**, *201*, 413.
(3) Burgman, P.; Nussenzweig, A.; Li, G. C. In *Thermoradiotherapy and Thermochemotherapy, Vol. 1: Biology, Physiology, Physics*; Seegenschmiedt, M. H., Fessenden, P., Vernon, C. C., Eds.; Springer: Berlin, 1995.
(4) Fairbairn, J. J.; Khan, M. W.; Ward, K. J. *Cancer Lett.* **1995**, *89*, 183.
(5) Song, C. W.; Choi, I. B.; Nah, B. S. In *Thermoradiotherapy and Thermochemotherapy, Vol. 1: Biology, Physiology, Physics*; Seegenschmiedt, M. H., Fessenden, P., Vernon, C. C., Eds.; Springer: Berlin, 1995.
(6) Multhoff, G.; Botzler, C.; Wiestnet, M. *Int. J. Cancer* **1995**, *61*, 272.
(7) Brezovich, I. A.; Meredith, R. F. *Hyperthermia* **1989**, *27*, 589.
(8) Brezovich, I. A.; Atkinson, W. J. *Med. Phys.* **1984**, *11*, 145.
(9) Case, J. A.; Tucker, R. D.; Park, J. B. *J. Biomed. Mater. Res. (Appl. Biomater.)* **2000**, *53*, 791.
(10) Stauffer, P. R.; Cetas, T. C.; Fletcher, A. M.; deYoung, D. W.; Dewhirst, M. W.; Oleson, J. R.; Roemer, R. B. *IEEE Trans. Biomed. Eng.* **1984**, *BME−31*, 76.
(11) Tucker, R. D.; Huidoboro, C.; Larson, T.; Platz, C. E. *J. Endourol.* **2000**, *14*, 511.
(12) Kimura, I.; Katsuki, T. *IEEE Trans. Magn.* **1986**, *MAG-22*, 1897.
(13) Takahashi, H.; Suda, T.; Motoyama, H.; Uzuka, T.; Takahashi, S.; Morita, K.; Kakinuma, K.; Tanaka, R. *Exp. Oncol.* **2000**, *22*, 186.
(14) Uzuka, T.; Tanaka, R.; Takahashi, H.; Kakinuma, K.; Matsuda, J.; Kato, K. *Int. J. Hyperthermia* **2001**, *17*, 114.
(15) Wiersma, J.; Van Dick, J. D. P. *Int. J. Hyperthermia* **2001**, *17*, 63.
(16) Andrä, W.; Dámbly, C. G.; Hergt, R.; Hilger, I.; Kaiser, W. A. *J. Magn. Magn. Mater.* **1999**, *194*, 197.
(17) Matsuki, H.; Satoh, T.; Murakami, K.; Hoshino, T.; Yanada, T.; Kikuchi, S. *IEEE Trans. Magn.* **1990**, *MAG-26*, 1551.

10.1021/cm011020i CCC: $22.00
Published on Web 12/15/2001

However, with regard to deeply seated malignant tumors, especially those of bone, hyperthermia is seldom performed because deep heating is technically difficult. In this sense, implants of bioactive ferromagnetic glass−ceramic are also able to generate heat in an alternating magnetic field. Moreover, these materials show the property of joining with the living tissues (essentially with bone tissue) by means of a strong chemical bond, when they are implanted into the body. The bioactive bond occurs due to the formation of an apatite-like layer on the tissue−implant interface during the first stages of the bioactive process.[22] The formation of the above-mentioned layer is characterized by several properties of the material (structural, textural, and chemical composition). Some "in vivo" experiments have been carried out, showing successful killing of cancerous cells in bone marrow and providing good bone integration.[23−25]

Luderer et al. showed that nonbioactive glass−ceramics containing lithium ferrites are useful as thermoseeds for hyperthermia treatment of cancer.[26] Afterward several papers have been published reporting the crystallization of magnetic (Fe_3O_4, α-Fe) together with bioactive and nonmagnetic phases.[27−30] By means of an adequate heat treatment, the magnetic properties have been improved because of the change in crystal size, although the bioactive behavior does not improve in all cases.[31] The presence of minority components in the initial glass composition (P_2O_5, B_2O_3, Na_2O) has been reported to be very important for the bioactive behavior of the glass−ceramic.[32]

The present work is a contribution to the field of magnetic and bioactive glass−ceramics. Until now, bioactive and magnetic glass−ceramics were based on two phases with different roles: one bioactive (such as wollastonite) and another with magnetic properties (magnetite, metallic iron, etc.). Increasing the amount of the first leads to a decrease of the properties provided by the second one. In this work, we present a new glass−ceramic based in $(Fe,Ca)SiO_3$ solid solution, in which magnetic and bioactive behavior should be provided by the same phase. Both properties will allow good bone integration and the possibility of using it as thermoseeds in hyperthermia treatment for localized tumors. The study of the magnetic and structural properties, as well as the in vitro behavior, will help us to understand the bioactivity process and heat generation after implantation into the living tissue.

Table 1. Ionic Concentration (mM) of Simulated Body Fluid and Human Plasma

	concentration (mM)			concentration (mM)	
ion	in SBF	in plasma	ion	in SBF	in plasma
Na^+	142.0	142.0	Cl^-	147.8	103.0
K^+	5.0	5.0	HCO_3^-	4.2	27.0
Mg^{2+}	1.5	1.5	HPO_4^{2-}	1.0	1.0
Ca^{2+}	2.5	2.5	SO_4^{2-}	0.5	0.5

Experimental Section

Synthesis of the Starting Glass. The glass, with nominal composition 45 mol % SiO_2, 45 mol % CaO, 10 mol % Fe_2O_3 and 3% by weight Na_2O, was obtained by melting and fast cooling of 8.112 g of SiO_2, 13.5 g of $CaCO_3$, 4.788 g of Fe_2O_3, and 1.126 g of Na_2CO_3. Na_2O was added to increase the reactivity and decrease the viscosity of the melting mixture. The raw materials mixture was introduced into a platinum crucible, heated from room temperature up to 800 °C at a heating rate of 10 °C/min, and maintained at this temperature for 3 h in order to remove the carbonates. From 800 °C up to 1400 °C the heating rate was 5 °C/min,g and that temperature was maintained for 30 min. The melt was cooled between two stainless steel plates at room temperature. The whole surface had a glassy appearance.

Synthesis of the Glass−Ceramics. The glass was milled into a vibrating mill for 24 h. The resulting powder was shaped in 600 mg disks of 12 mm diameter × 1.5 mm height, by means of uniaxial (1.5 tons) and isostatic pressure (5 tons).

The disks of glass were heated to 800 °C at a rate of 5 °C/min, maintained at this temperature for 3 h, and cooled to room temperature. The process was performed in N_2 atmosphere to avoid the formation of hematite (α-Fe_2O_3), a nonmagnetic phase. The disk surfaces were polished with SiC and characterized by X-ray diffraction (XRD) and scanning electron microscopy (SEM) coupled to X-ray dispersive energies spectroscopy (EDX) (JEOL 6400-LINK AN 10000 microscope). X-ray patterns were obtained using a Philips X'Pert MDP (Cu Kα radiation) diffractometer; the patterns were made using $\theta-2\theta$ as well as grazing incidence with an angle of 0.5°. The thermogravimetric and differential thermal analyses (TG/DTA) were carried out between 30 and 1000 °C in N_2 (flow rate 100 mL/min at a heating rate of 5 °C/min), using a Seiko TG/DTA 320. The magnetic characterization was carried out using a SQUID magnetometer (Quantum Design, MPMS-XL). Mössbauer experiments were performed in air at room temperature, using a Co source in a Rh matrix. The isomer shift values are given relative to the center of the α-Fe spectrum.

In Vitro Bioactivity Test. A bioactive material is one that allows a specific biological response at its interface, enabling the formation of links between the tissues and said material.[33] The "bioactive bond" takes place by means of an apatite-like layer formed on the surface, when the implant is in contact with the physiological fluids. This property is tested in vitro by soaking the material in a simulated body fluid (SBF)[34] with an ionic concentration similar to that of human plasma (Table 1). For this purpose the disks were soaked in 50 mL of SBF at 37 °C, inside sterile polyethylene recipes, held in the vertical position by platinum wires to avoid precipitation on the surface (Figure 1). The SBF was filtered (Millipore, 0.23 μm), and

(18) Chan, D. C. F.; Kirpotin, D. B.; Bunn, P. A., Jr. *J. Magn. Magn. Mater.* **1993**, *122*, 374.
(19) Shinkai, M.; Yanase, M.; Suzuki, M.; Honda, H.; Wakabayashi, T.; Yoshida, J.; Kobayashi, T. *J. Magn. Magn. Mater.* **1999**, *194*, 176.
(20) Jordan, A.; Scholz, R.; Wust, P.; Schirra, H.; Schiestel, T.; Schmidt, H.; Felix, R. *J. Magn. Magn. Mater.* **1999**, *194*, 185.
(21) Hiergeist, R.; Andra, W.; Buske, N.; Hert, R.; Hilger, I.; Rechter, U.; Kaiser, W. *J. Magn. Magn. Mater.* **1999**, *201*, 420.
(22) Hench, L. *J. Am. Ceram. Soc.* **1998**, *81*, 1705.
(23) Ikenaga, I.; Ohoura, K.; Nakamura, T.; Kotoura, Y.; Yamamuro, T.; Oka, M.; Ebisawa, Y.; Kokubo, T. *Bioceramics* **1991**, *4*, 255.
(24) Ohura, K.; Ikenaga, M.; Nakamura, T.; Yamamuro, T.; Ebisawa, Y.; Kokubo, T.; Kotoura, Y.; Oka, M. *J. Appl. Biomater.* **1991**, *2*, 153.
(25) Ikenaga, M.; Ohura, K.; Yamamuro, T.; Kotoura, Y.; Oka, M.; Kokubo, T. *J. Orthop. Res.* **1993**, *6*, 849.
(26) Lurderer, A. A.; Borreri, N. F.; Panzarino, J. N.; Mansfield, G.; Hess, D. M.; Brown, J. L.; Barnell, E. H. *Radiat. Res.* **1983**, *94*, 190.
(27) Ebisawa, Y.; Miyaji, F.; Kokubo, T.; Ohura, K.; Nakamura, T. *J. Ceram. Soc. Jpn.* **1997**, *105*, 947.
(28) Konaka, H.; Miyaji, F.; Kokubo, T. *J. Ceram. Soc. Jpn.* **1997**, *105*, 833.
(29) Lee, Y. K.; Kim, K. N.; Choi, S. Y.; Kim, C. S. *J. Mater. Sci., Mater. Med.* **2000**, *11*, 511.
(30) Singh, K.; Bahadur, D. *J. Mater. Sci., Mater. Med.* **1999**, *10*, 481.
(31) Ebisawa, Y.; Sugimoto, Y.; Hayashi, T.; Kokubo, T.; Ohura, K.; Yamamuro, T. *Nippon Seramikkusu Kyokai Gakujutsy Ronbunshi* **1991**, *99*, 7.
(32) Ebisawa, Y.; Miyaji, F.; Kokubo, T.; Ohura, K.; Nakamura, T. *Biomaterials* **1997**, *18*, 1277.
(33) Hulbert, S. F.; Hench, L. L.; Forbers, D.; Bowman, L. S. *Ceram. Int.* **1982**, *8*, 121.
(34) Kokubo, T.; Kushitani, H.; Sakka, S.; Kitsugi, T.; Yamamuro, T. *J. Biomed. Mater. Res.* **1990**, *24*, 721.

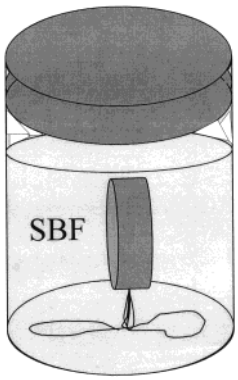

Figure 1. Scheme of the "in vitro" bioactivity test. The disk is held vertically to avoid precipitation on its surface.

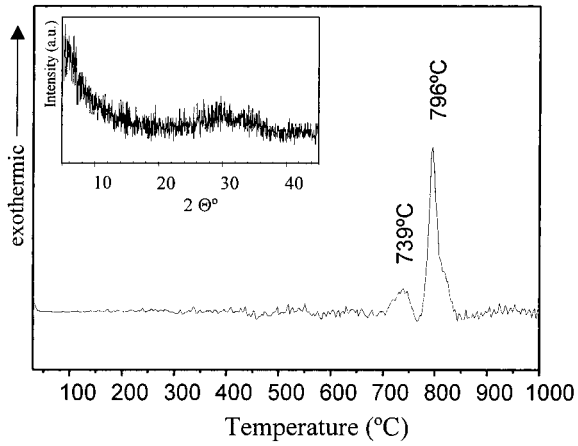

Figure 2. ATD diagram carried out over the starting glass. The inset shows the XRD pattern of the starting glass.

every operation was carried out under laminar flux (Telstar AV-100) to avoid bacterial contamination. After 20 days and 40 days, the disks were removed from the SBF and their surfaces were studied by XRD, SEM, and EDX. The experiment was carried out in duplicate, that is, with two pieces for each soaking time. XRD and SEM observations were very reproducible. Three EDX experiments were performed on each sample.

To study the ionic exchange between the SBF and the sample, the changes in the SBF of pH and Ca^{2+} concentration were determined by means of a Na^+, K^+, Ca^{2+}, pH Ilyte system. The concentrations of P, Fe, and SiO_2 in the SBF were determined by UV−vis spectrophotometry (Unicam UV 500), using Spinreact, Ferrimat-Kit, and Nanocolor tests, respectively.

Results and Discussion

The melting process led to an amorphous glass without detectable crystalline phases when it is observed by XRD (inset of Figure 2). DTA carried out over the glass (Figure 2) shows two exothermic processes, with maxima at 739 and 796 °C. Both peaks are assigned to the crystallization of two different phases due to the thermal treatment. Taking into account these results, the initial glass was heated to 800 °C in order to obtain a glass−ceramic, as was described above.

Figure 3a shows the XRD pattern of the glass−ceramic obtained under $\theta-2\theta$ conditions. The diffraction maxima can be assigned to a majority wollastonite phase and a minority ϵ-$CaSiO_3$ phase. The presence of these crystalline phases agrees with the two exothermic processes observed by DTA. The width of the maxima

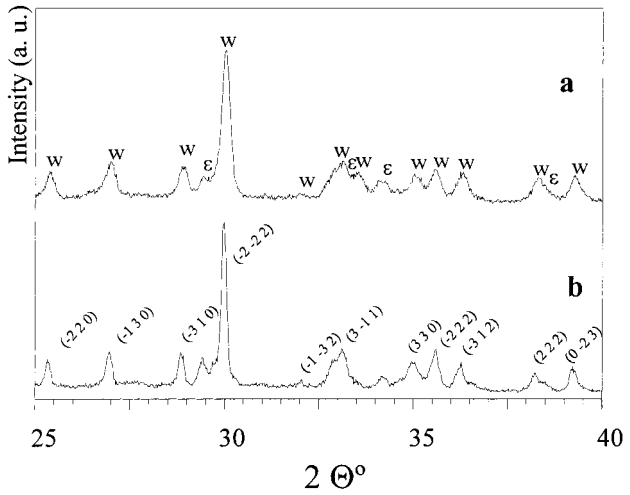

Figure 3. XRD patterns of the glass−ceramic using $\theta-2\theta$ collection: (a) before soaking; (b) after soaking for 40 days; (W) wollastonite-like phase; (ϵ) ϵ-$CaSiO_3$ phase. Miller's indexes are assigned for the wollatonite phase.

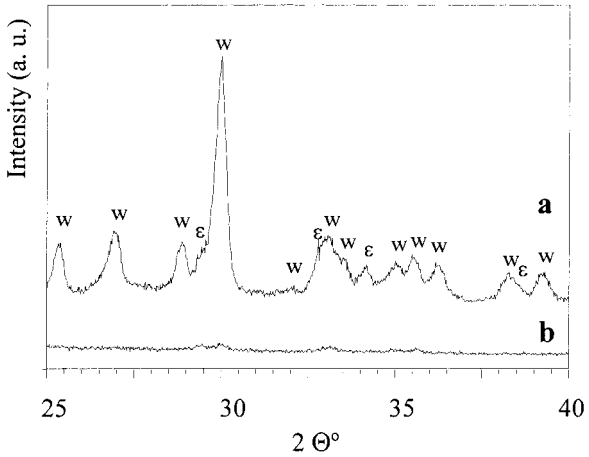

Figure 4. XRD patterns of the glass−ceramic using grazing incidence: (a) before soaking; (b) after soaking for 40 days; (W) wollastonite-like phase; (ϵ) ϵ-$CaSiO_3$ phase.

suggests that both phases are made up of small size crystallites. The average size of the crystallites were calculated by the Debye−Scherrer method, obtaining values of about 50 nm for both phases. No maxima corresponding to magnetite, α-Fe_2O_3, or any other iron oxide can be observed by XRD.

In Vitro Bioactivity Test. The XRD pattern shown in Figure 3b corresponds to that of the glass−ceramic sample after being soaked in SBF during 40 days obtained under identical conditions to those for the ab initio glass−ceramic (Figure 3a). The same phases obtained before soaking can be observed, but with a slight narrowing of the maxima; this suggests an increase of the crystallites size, which could be due to an aging of the glass−ceramic crystallites under the in vitro test conditions.

Figure 4 shows the XRD patterns using grazing incidence of the same samples described in Figure 3. Substantial differences can be observed with regard to the phases at the surface. Before being soaked in SBF, the glass−ceramic surface shows the same crystalline phases as the bulk (Figure 3a). However, after 40 days of soaking in SBF, no reflection appears, suggesting that a layer, amorphous for XRD, has coated the surface.

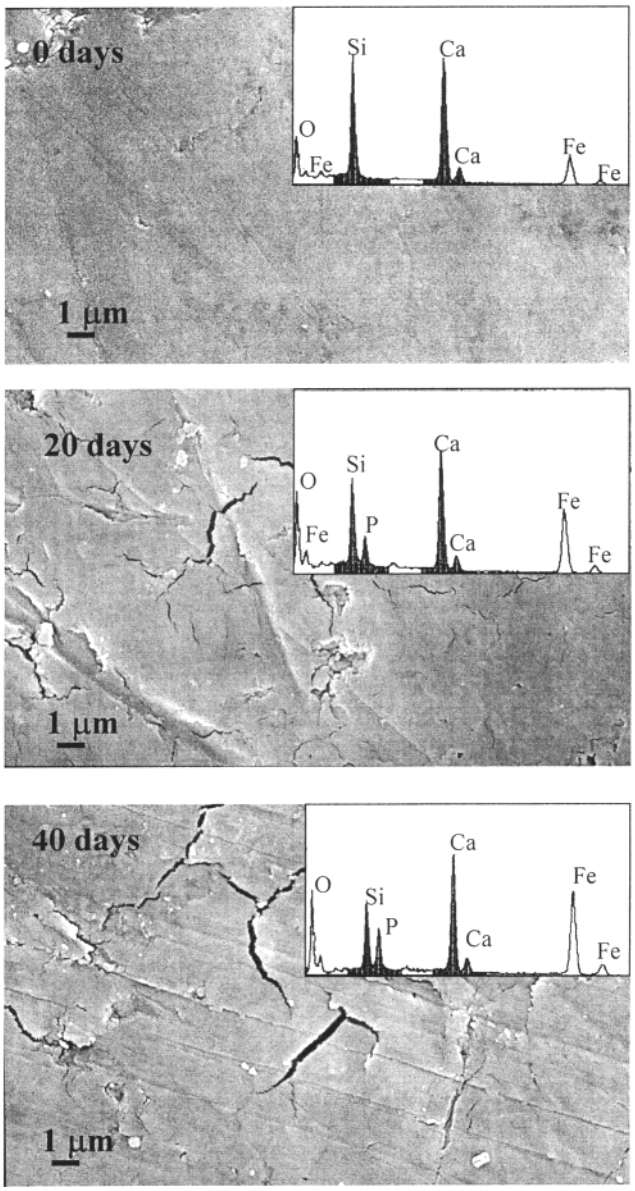

Figure 5. Micrographs obtained by SEM of the glass−ceramic before (0 days) and after being soaked in SBF (20 and 40 days). The insets show the EDX spectra obtained for the glass−ceramic surface.

Figure 5 shows the SEM micrographs of the sample surfaces before (0 days) and after being soaked in SBF for 20 and 40 days. The images include the chemical composition of the surface obtained by EDX. The micrograph of the sample before being soaked shows the typical smooth surface of the polished glass−ceramics, with a few defects created by the synthesis process. The EDX analysis shows a chemical composition of the surface that corresponds to the nominal composition of the bulk (see Table 2).

After being soaked 20 days, a change in the chemical composition of the surface can be noticed. The most relevant fact is the appearance of phosphorus, together with the decrease of the silicon concentration and the increase of iron. The SEM micrograph shows cracks; they could be formed either during the metalation process under vacuum or because of the electron beam during the observation process. These cracks do not appear at the surface of the nonsoaked sample (0 days); this suggests that what is cracking is the newly formed

Table 2. Chemical Composition (atom %) of the Glass−Ceramic Surface before and after Being Soaked in SBF

	composition (atom %)		
element	0 days	20 days	40 days
Si	41	30	18
Ca	40	32	28
Fe	19	31	42
P		7	12

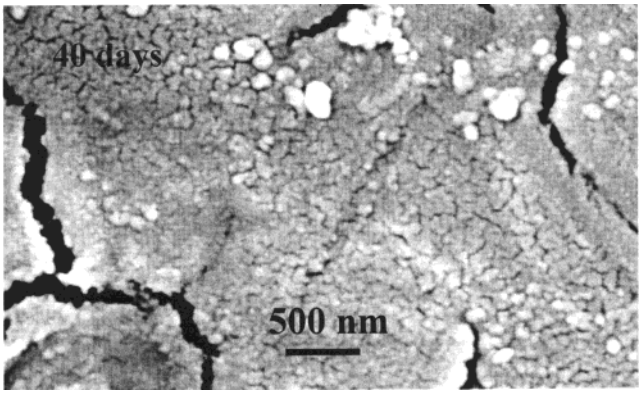

Figure 6. Micrograph obtained by SEM of the glass−ceramic after being soaked in SBF for 40 days. Magnification ×25000.

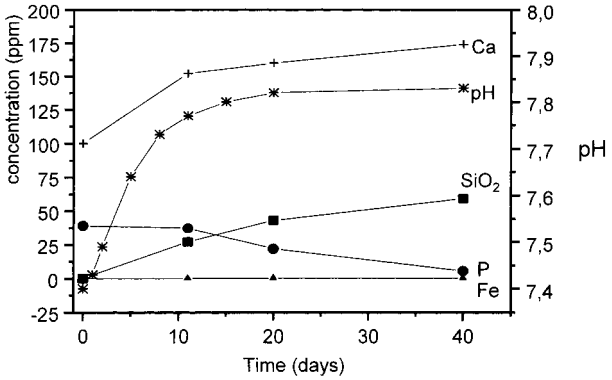

Figure 7. Changes of pH and SBF composition as a function of soaking time.

layer on the surface of the glass−ceramic, grown as a consequence of the reactivity of the glass−ceramic surface with the SBF. This layer would avoid the observation of the XRD maxima of the glass−ceramic when it is measured by grazing incidence (Figure 4b).

The composition changes slightly in relation to that of the sample soaked for 20 days when the soaking time in SBF increases to 40 days. With regard to the amorphous layer width, it is supposed to increase because the cracks are larger and deeper.

Figure 6 shows a micrograph of the sample soaked for 40 days, obtained with a higher magnification (×25000). This micrograph allows us to observe the texture of the growth amorphous layer, as well as a few isolated particles and groups of spherical particles with diameters ranging in size between 50 and 200 nm.

Figure 7 shows the SBF composition as a function of soaking time; a Ca^{2+} and SiO_2 exchange occurs from the samples to the SBF, coinciding with a pH increase from 7.4 to 7.84. Both processes are more intense during the first 10 days, and after this time the increase is lower. Likewise, after 40 days the SiO_2 exchange from the sample to SBF can be estimated to be around 1.4% of

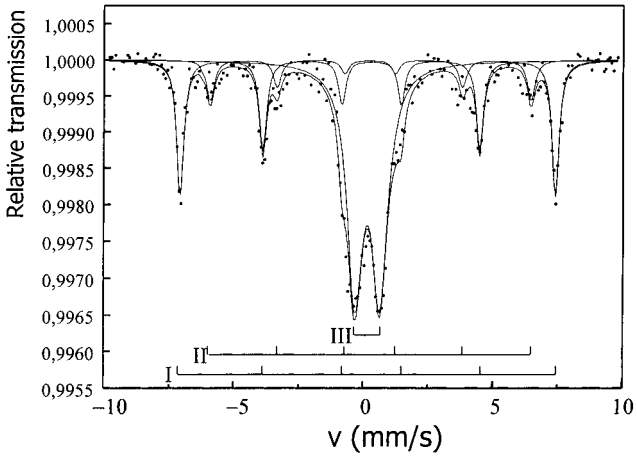

Figure 8. Fe^{57} Mössbauer spectrum of the glass−ceramic obtained at room temperature: subspectrum I, six-line spectrum assigned to Fe^{2+} in ferroan−wollastonite; subspectrum II, six-line spectrum assigned to Fe^{2+} in ϵ-$(Fe,Ca)SiO_3$; subspectrum III, two-line spectrum assigned to Fe^{3+} in the paramagnetic glassy matrix.

the total amount of the sample content. The phosphorus content of the SBF decreases after 10 days, that is, after the rapid process of Ca^{2+} transfer and pH increase. After 40 days the phosphorus content in the SBF decreases around 90%. The theory proposed by Kokubo[34] for SiO_2−CaO based bioactive materials says that an ionic exchange between Ca^{2+} and H_3O^+ takes place when a bioactive material is in contact with physiological fluids. Such an exchange produces the formation of silanol groups (Si−OH) on the surface, inducing the formation of an amorphous calcium phosphate and, after the subsequent crystallization, an apatite-like phase, by means of the incorporation of phosphorus and calcium from the fluid. The cationic exchange of calcium between the glass−ceramic and the SBF, the pH increase, and the amorphous layer growth by phosphorus incorporation observed in our glass−ceramic agree with the first stages of this theory. The crystallization of apatite could not be confirmed by XRD because the nanocrystal size is lower than 20 nm[35] in this stage of the bioactive process. The formation of such a coating could enable the regeneration and bone integration when implanted in the living tissue.[36]

Finally, the amount of iron transferred from the sample to the SBF is small (7 ppm at the end of the test), which implies an almost constant iron content in the glass−ceramic after being soaked for 40 days. The increase of the iron amount on the surface of the sample can be noticed. During the lixiviation process, the silicon and calcium compounds are eluted to the medium but the iron ones remain, which seems to suggest that iron is taking part of the nonsoluble compounds for the test conditions. This could be the reason for the increment of iron on the surface of the sample where the EDX results would be the sum of two factors: the nonsolubility of the iron compounds and therefore the higher iron concentration with respect to the silicon and calcium initial relative values, and the tiny thickness of the new formed layer which is crossed by the beam.

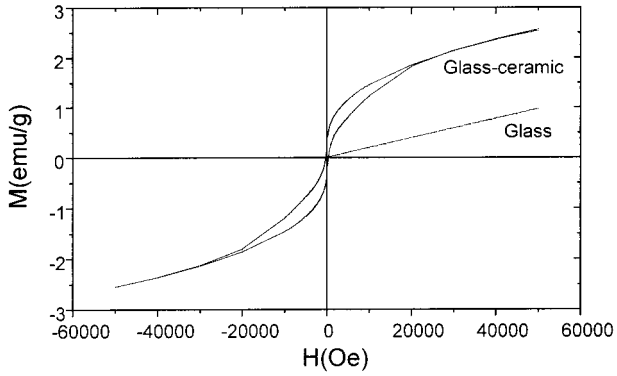

Figure 9. Hysteresis loops of the starting glass and glass−ceramic obtained at room temperature.

Table 3. Mössbauer Parameters Obtained for the Glass−Ceramic

subspectrum	isomer shift (mm/s)	hyperfine field (kOe)	peak width (mm/s)	subspectrum area (%)
I	0.237	448	0.311	31.5
II	0.246	381	0.350	10.3
III	0.159		0.750	58.2

Magnetic Properties. The Mössbauer spectrum for the glass−ceramic is shown in Figure 8. The spectrum was fitted to one doublet and two six-line spectra. The doublet shows the existence of a paramagnetic phase in the glass−ceramic. The value of its quadropole splitting is 0.97, pointing out that only Fe^{3+} constitutes this phase (no paramagnetic Fe^{2+} is detected in the spectrum). Moreover, the peak width of this subspectrum (Table 3) indicates that this phase is placed into a glassy or nanocrystalline environment.

The six-line subspectra point out that there are two magnetically ordered phases in the glass−ceramic. The isomer shifts do not correspond either with Fe^{2+} or Fe^{3+} placed into the magnetite structure.[37,38] These data together with XRD data confirm the absence of magnetite in our glass−ceramic.

Subspectrum I (Figure 8) is a six-line spectrum which provides 31.5% of the relative integrated area, while the other six-line spectrum (subspectrum II) provides 10.3%. The presence of two ordered magnetic phases is clear, and the relative areas could be an estimation of the relative amount of iron in each phase. Considering the XRD patterns, we assign subspectra I and II to the ferroan−wollastonite and $\epsilon(Fe,Ca)SiO_3$, respectively. Moreover, the paramagnetic component (subspectrum III) provides 58.2% of the relative area, showing the presence of an important amount of paramagnetic iron.

The magnetization curve of the glass is shown in Figure 9. The paramagnetic behavior indicates that, during the fabrication process, no magnetic phase has appeared. The hysteresis loop of the sample heat-treated at 800 °C during 3 h is also shown in Figure 9; the difficulty to reach the saturation magnetization can be noticed. The value of the magnetic moment is small because of the low content of iron, and the coercive force is about 300 Oe. The hysteresis loop profile shows, because of its shape, the presence of at least two ferromagnetic phases with different coercive forces. The

(35) Vallet-Regí, M.; Izquierdo-Barba, I.; Salinas, A. J. *J. Biomed. Mater. Res.* **1999**, *46*, 560.
(36) Vallet-Regí, M. *J. Chem. Soc., Dalton Trans.* **2001**, 97.
(37) Kurkjian, C. R. *J. Non-Cryst. Solids* **1970**, *3*, 157.
(38) Sawatzky, G. A.; Van der Woude, F.; Morrish, A. H. *Phys. Rev.* **1969**, *187*, 747.

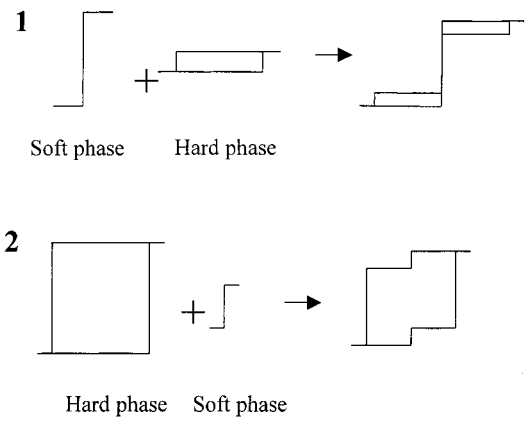

Figure 10. Schemes of the resulting hysteresis loops by combination of (1) a predominant soft magnetic phase over a hard magnetic phase and (2) a predominant hard magnetic phase over a soft magnetic phase.

hysteresis loop can be fitted as a combination of two loops. In Figure 10 two different possibilities are outlined without considering other magnetic parameters: (1) the softer phase and (2) the harder phase as the predominant one. Figure 10 shows that our loop fits the first model; that is, the softer phase predominates over the harder one.

It is well-known that glasses based on the $SiO_2-CaO-Fe_2O_3$ system contain Fe^{2+} and Fe^{3+}, with a higher amount of Fe^{3+}.[29] In another way, the crystallization temperature for magnetite in this system has been reported to be about 900 °C.[31] We treated the starting glass at 800 °C, which is not a high enough temperature for crystallizing magnetite into the glassy matrix. However, 800 °C could be high enough to incorporate the Fe^{2+} fraction into the crystallized calcium silicates. Therefore, we would obtain a solid solution like ferroan−wollastonite, where Fe(II) would be placed into the octahedral sites M1, M2, and M3[39] and a second ϵ-(Ca,Fe)SiO_3-like phase. Fe^{3+} cannot be incorporated into these solid solutions because of its oxidation state, remaining in a paramagnetic state in the amorphous matrix.

$Fe_2O_3-CaO-SiO_2$ starting glasses, containing 40% (wt) α-Fe_2O_3 as raw material, lead to the formation of magnetite and β-wollastonite after thermal treatment.[31] However, other glasses based on $SiO_2-Na_2O-Fe_2O_3-CaO-P_2O_5-B_2O_3$ with Fe_2O_3 contents between 5 and 15% and high contents of sodium lead to $Na_{3-x}Fe_xPO_4$ solid solutions, without magnetite in the glass−ceramic.[30] Our glass−ceramic, with 10% α-Fe_2O_3, seems to be like the second case. No iron oxides (such as Fe_3O_4, γ-Fe_2O_3, α-Fe_2O_3, etc.) are present in it; therefore, Fe^{2+} ions have to stay, forming a solid solution with the crystalline phases and Fe^{3+} ions in the noncrystallized amorphous matrix fraction of the glass−ceramic.

The presence of ferroan−wollastonite and ϵ-(Ca,Fe)-SiO_3 phases explains the two different phases for the ferromagnetic iron in the Mössbauer spectra, as well as the presence of two different magnetic phases deduced by the hysteresis loop profile. The XRD patterns show that the wollastonite-like phase is the predominant one, while the ϵ-$CaSiO_3$-like phase is the minor one. These data and the hysteresis loop point out that the ferroan−wollastonite is the predominant and softer phase. However, from those data it cannot be distinguished whether the magnetization process is due to wall movements or to the existence of single domain particles.

Besides, the paramagnetic phase explains the difficulty to reach the saturation magnetization of the sample. This is the major contribution in this region of the hysteresis loop. We can identify the slope of the graph and the susceptibility in emu/g·Oe. For the region of high field

$$\chi_g/\chi_{g-c} = N_g m_g^2/N_{g-c} m_{g-c}^2$$

where N_g is the number of iron ions in 1 g of the glass sample, m_g is the magnetic moment of 1 g of the glass sample, N_{g-c} is the number of iron ions in 1 g of the glass−ceramic sample, and m_{g-c} is the magnetic moment of 1 g of the glass sample. Since N_{g-c} is smaller than N_g (some amount of Fe ions get out to the paramagnetic glassy phase to constitute the ferromagnetic nanocrystalline phases) and the slopes of the glass and the glass−ceramic in the approach to saturation seem to be similar ($\chi_g/\chi_{g-c} \sim 1$), then m_{g-c} has to be higher than m_g. In other words, the effective magnetic moment of the paramagnetic phase of the glass−ceramic has to be higher than the effective magnetic moment of the glass before the heat treatment. This agrees with the fact that only Fe^{3+} (which has a higher magnetic moment than Fe^{2+}) would remain in the amorphous phase after the heat treatment.

As the electric resistivity of the material is supposed to be high, the heat will be generated in an amount proportional to the area of the hysteresis loop and the frequency of the alternating applied magnetic field. This heat could be used to kill the cancerous cells around the material after it has been implanted into the cancerous bone. In vivo experiments with magnetite−wollastonite glass−ceramics[23] have shown that magnetic fields of 300 Oe at 100 kHz were able to generate 10 W·g^{-1}. Although our material is quite different with respect to the magnetic phases included, the applied field to achieve sufficient heating could be similar to that mentioned above.

Patients treated by curettage of bone tumors need reinforcement of the weakened bone after the surgery. Moreover, even if curettage is well performed, having a remainder of some malignant cells is very possible. A bioactive glass−ceramic, if it generates heat, could be used to treat bone tumors and reinforce the weakened tumor bone. Ferrofluids, or typical thermoseeds (such as wires of metal alloys), have shown good hyperthermic performance against several tumors, mainly in combination with other therapies.[40] However, these kinds of methods do not provide the orthopaedic possibilities proposed with our material. The features of this glass−ceramic allow many possibilities in regard to this topic. By increasing the iron content in the composition or by increasing the temperature of the thermal treatment, we can obtain glass−ceramics with higher heating power. In another way, these changes would decrease the material bioactivity. Depending on the different

(39) Ohashi, Y.; Finger, L. W. *Am. Mineral.* **1978**, *63*, 274.

(40) Falk, M. H.; Issels, R. D. *Int. J. Hyperthermia* **2001**, *17*, 1.

necessities of the patients, this material can be modified in one way or another.

Conclusions

(1) A $SiO_2-CaO-Fe_2O_3-Na_2O$ based glass−ceramic, suitable to be used as a biomaterial for bone substitution, has been obtained.

(2) A coating, amorphous according to XRD, is induced on the sample surface when soaked in SBF. This coating occurs by taking phosphorus from the solution.

(3) This glass−ceramic shows magnetic properties, useful for the hyperthermia treatment of localized tumors. The magnetic properties are due to mixed $(Fe,Ca)SiO_3$ phases with different structures: wollastonite and ϵ-$CaSiO_3$.

(4) This kind of compound allows different possibilities to improve its magnetic properties: by increasing the thermal treatment and increasing the iron content. A balance between the bioactivity and the magnetism should be found.

Acknowledgment. Financial support of CICYT, Spain, through research project MAT99-0466 is acknowledged. R.P.d.R. is grateful to Consejería de Educación y Cultura (C.A.M.). We also thank A. Rodriguez (Electron Microscopy Center, Complutense University), F. Conde (C.A.I. X-ray Difracction, Complutense University), and P. Agudo (Applied Magnetism Institute, RENFE-UCM) for the valuable technical and professional assistance.

CM011020I